J|A|C|S
COMMUNICATIONS

Published on Web 07/10/2002

Active-Site Stereochemical Control of Oxygen Atom Transfer Reactivity in Sulfite Oxidase

Katrina Peariso, Rebecca L. McNaughton, and Martin L. Kirk*

Contribution from The Department of Chemistry at The University of New Mexico, Albuquerque, New Mexico 87131-1096

Received October 2, 2001

Understanding how an oxygen atom is transferred between a substrate and a transition metal is of fundamental chemical and biological interest. Recently, there has been significant progress in studies directed toward understanding the mechanism of oxygen atom transfer (OAT) in small-molecule analogues of the pyranopterin molybdenum enzymes including sulfite oxidase (SO). Sulfite oxidase is found in the mitochondrial intermembrane space of vertebrates, where the physiologically important oxidation of sulfite is the terminal step in the oxidative degradation of Cys and Met.[1−4] The consensus structure of the catalytically competent oxidized Mo(VI) active site in SO is five-coordinate square pyramidal, possessing two terminal oxo ligands, an ene-1,2-dithiolate, and a catalytically essential Cys sulfur donor.[5−8] X-ray crystallography reveals that the substrate (solvent) access channel is in the ene-1,2-dithiolate plane of the active site,[5] indicating that the equatorial oxo ligand (O_{eq}) is the catalytically labile oxo ligand involved in the oxidation of sulfite. Herein, we propose that O-atom activation *and* selection in SO is not primarily facilitated by direct interaction with substrate or the orientation of the Cys thiolate. Rather, O-atom selection and activation are a direct function of the low-symmetry structure of the oxidized active site. The O_{ax} has no trans ligand, while O_{eq} is trans to a dithiolate S, indicating a role for the ene-1,2-dithiolate in promoting OAT reactivity via a kinetic trans effect.

Using $[MoO_2(dithiolate)_2]^{2-}$ complexes, Holm and co-workers[9] have proposed a mechanism for the thermodynamically favorable OAT reaction from dioxomolybdenum complexes to a tertiary phosphine which shows that the initial steps in the OAT sequence occur via an associative mechanism. Support for an associative mechanism has been described by Smith et al.,[10] who were able to isolate and characterize [(L-N_3)MoO(OPh)($OPEt_3$)], an intermediate in the OAT reaction between [(L-N_3)MoO_2(OPh)] and triethylphosphine. This intermediate displays a lengthening of the phosphine−O bond and a shortening of the terminal Mo−O bond, demonstrative of the "spectator oxo" effect described by Rappé and Goddard.[11] The spectator oxo effect caused by substrate binding yields two distinct Mo−O distances; the Mo═O at 1.67 Å and Mo−O···P at 2.18 Å. These results show that substrate attack provides for oxo selection by weakening the active Mo−O bond, allowing the spectator oxo to form a stronger Mo−O bond with a formal bond order of three. Along these lines, Hall and co-workers[12,13] have performed calculations on higher-symmetry (C_2) dioxomolybdenum model complexes and have proposed a catalytic mechanism (Scheme 1) for the two-electron oxidation of sulfite that involves initial attack of the sulfur lone pair on one of the two oxo donors to generate a $2e^-$ reduced Mo(IV) product-bound species.

Ligand-field induced dioxomolybdenum symmetry breaking has been suggested as a means of oxo selection by Izumi et al.[14] in detailed spectroscopic and computational studies of [(L-N_3)Mo^{VI}-O_2(SCH_2Ph)]. They proposed that breaking the degeneracy of the

Scheme 1

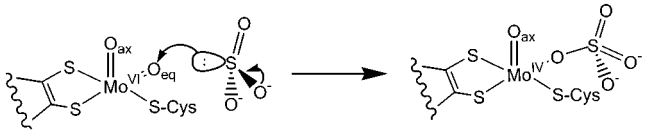

two Mo═O π^* acceptor orbitals effectively activates or selects a specific oxo group for transfer to the substrate, and this selection is a function of the O−Mo−$S_{thiolate}$−C torsion angle which modulates the overlap of a S p orbital with one of the Mo═O π^* orbitals. This is a remarkable observation that implies the dihedral angle of the coordinated Cys in SO may orient the S_{Cys}p orbital to select O_{eq} for transfer to sulfite. Collectively, studies on the model systems indicate that the *activation* of a given oxo ligand for transfer to substrate is initiated by either the initial interaction of substrate with an active-site oxo ligand[9,12,13] (pre-transition state) or the orientation of the S_{Cys}p orbital relative to the two oxo ligands[14], or both.

We have performed electronic structure calculations[15] at the DFT level of theory[16] on $[Mo(VI)O_2(S_2C_2Me_2)(SCH_3)]^-$, a computational model of the oxidized SO site (SO_{ox}), and the results strongly suggest that the two oxo ligands are highly *inequivalent* electronically. Figure 1 depicts an electron density contour plot of the $[Mo(VI)O_2(S_2C_2Me_2)(SCH_3)]^-$ LUMO, which is the putative electron acceptor orbital in the OAT reaction with the sulfite substrate. Inspection of the LUMO indicates that it is principally comprised of a d−p π^* antibonding interaction between the Mo d_{xy} orbital and an O_{eq} p orbital, which respectively contribute 52% and 20% of the total atomic orbital character to this molecular orbital. In stark contrast, the axial oxo (O_{ax}) possesses essentially no contribution to this orbital. Thus, the unique geometry of the SO_{ox} site determines the precise nature of the LUMO, and plays a defining role in both the selection and activation of the O_{eq} toward O-atom acceptors.

O-atom selection is incurred by the fact that the lowest-energy acceptor orbital (LUMO) is highly stabilized (≥0.9 eV) with respect to the lowest-energy virtual orbital (LUMO+1) which possesses appreciable O_{ax} orbital character (see Figure S1). The large energetic stabilization of the LUMO, coupled with favorable overlap between the sulfite HOMO and the O_{eq} p orbital of the LUMO, facilitates substrate attack at this position. The activation of the equatorial oxo is also a function of the trans-effect of the equatorial dithiolate S on the O_{eq}, as the Mo═O_{eq} bond order is now formally 2, instead of 2.5 as observed in $[MoO_2]^{2+}$ complexes where the two terminal oxo ligands are symmetry-related. A reduction in the activation energy for the OAT process undoubtedly results from the nature of the heterodinuclear Mo═O_{eq} d−p π^* interaction which, when occupied by the sulfite lone pair, facilitates cleavage of the Mo═O_{eq} bond and promotes product release. Thus, the unique electronic

10.1021/ja017217t CCC: $22.00 © 2002 American Chemical Society

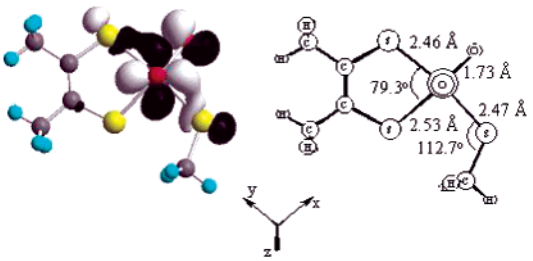

Figure 1. Molecular orbital isosurface of the $[Mo(VI)O_2(S_2C_2Me_2)(SCH_3)]^-$ LUMO (left) and a schematic representation of the optimized active site (right). Both representations are oriented looking down the axial oxo donor. The optimized $Mo-O_{ax}$ distance is 1.71 Å and the $O_{ax}-Mo-S_{thiolate}-C$ torsion angle is 73° (as compared with ~90° determined from the SO crystal structure). For a more extensive list of the optimized parameters see Table S1.

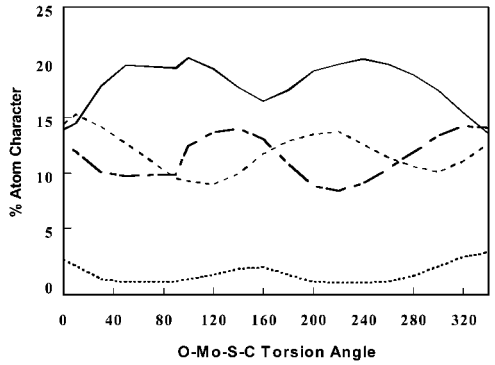

Figure 2. Plot of the contributions of O_{eq} (solid line), O_{ax} (dotted line), $S_{thiolate}$ (dashed line), and $S_{dithiolene}$ (dot−dash line) to the total orbital character of the LUMO as a function of the $O_{ax}-Mo-S_{thiolate}-C$ torsion angle.

structure imposed by the low symmetry of the SO active site may contribute substantially to the difference between the OAT rate of the enzyme compared to that of early model systems. We are currently working to quantitate the effect of the energetic stabilization observed for the LUMO on the kinetics of sulfite attack on O_{eq}.

To assess the role of the coordinated Cys on the OAT process, we examined the effect of the $O_{ax}-Mo-S_{Cys}-C$ torsion angle on the atomic orbital character of the LUMO, and the results of these calculations are presented in Figure 2. While the thiolate S^v p orbital character oscillates in a sinusoidal manner as the torsion angle changes, reflecting the differential overlap of the S^v p orbital with Mo d_{xy}, there is no appreciable change in the orbital character of O_{eq} or O_{ax} as a function of the $O_{ax}-Mo-S_{Cys}-C$ torsion angle. Thus, in apparent contrast to analogous computational studies on dioxomolybdenum model compounds which lack a coordinated ene-1,2-dithiolate,[14] it appears that the coordinated Cys in SO does not function to select the oxo atom that is being transferred to the substrate.

Mutation-induced changes in the active-site electronic structure of SO may be a primary basis for human isolated sulfite oxidase deficiency, which derives from specific mutations in the SO gene.[17] A208 is highly conserved in SO enzymes from a variety of organisms and is located on the N-terminal side of the C207 donor in humans. It is interesting to speculate how the A208D mutation affects the $Mo-S_{Cys}$ interaction in the mutant enzyme. It can be expected that the larger, charged D208 residue induces steric crowding in the Mo binding pocket, distorting the 84° $O_{axial}-Mo-S_{thiolate}-C$ torsion angle found in the wild-type enzyme.[5] The results presented here argue against these modifications affecting the OAT half reaction, providing the mutation still allows substrate access to the active site. This suggests that, while the $O_{ax}-Mo-S_{Cys}-C$ torsion angle does not contribute to oxo selection, it may control the reduction potential of the reduced *mono-oxomolybdenum* SO site[18] and play a critical role in electron transfer regeneration of the oxidized SO center. We are currently engaged in spectroscopic studies of relevant dioxomolybdenum model[19] and enzyme systems directed toward experimentally calibrating the computational results presented herein and determining how the equatorial Cys thiolate is coupled into the d_{xy} redox orbital of the reduced SO in order to understand the role of this critical ligand in the enzyme mechanism.

Acknowledgment. This work was supported by a Grant from the National Institutes of Health (GM-057378) to M.L.K. K.P. is supported by an NRSA Postdoctoral Fellowship (DK59724) from the NIH.

Supporting Information Available: Table comparing the relevant geometric parameters of the optimized computational model with the crystal structure of sulfite oxidase and $(Et_4N)[MoO_2(SC_6H_2\text{-}2,4,6\text{-}Pr^i_3)(bdt)]$ and the initial coordinates; a plot of the orbital energies of the Mo d-orbital manifold with their respective electron density isosurfaces (PDF). This material is available free of charge via the Internet at http://pubs.acs.org.

References

(1) Hille, R. *Chem. Rev.* **1996**, *96*, 2757−2816.
(2) Spiro, T. G.; Ed. *Molybdenum Enzymes*; John Wiley and Sons: New York, 1985.
(3) Cohen, H. J.; Fridovich, I. *J. Biol. Chem.* **1971**, *246*, 359−366.
(4) Cohen, H. J.; Fridovich, I.; Rajagopalan, K. V. *J. Biol. Chem.* **1971**, *246*, 374−382.
(5) Kisker, C.; Schindelin, H.; Pacheco, A.; Wehbi, W. A.; Garrett, R. M.; Rajagopalan, K. V.; Enemark, J. H.; Rees, D. C. *Cell* **1997**, *91*, 973−983.
(6) George, G. N.; Kipke, C. A.; Prince, R. C.; Sunde, R. A.; Enemark, J. H.; Cramer, S. P. *Biochemistry* **1989**, *28*, 5075−5080.
(7) George, G. N.; Garrett, R. M.; Prince, R. C.; Rajagopalan, K. V. *J. Am. Chem. Soc.* **1996**, *118*, 8588−8592.
(8) Garrett, R. M.; Rajagopalan, K. V. *J. Biol. Chem.* **1996**, *271*, 7387−7391.
(9) Tucci, G. C.; Donahue, J. P.; Holm, R. H. *Inorg. Chem.* **1998**, *37*, 1602−1608.
(10) Smith, P. D.; Slizys, D. A.; George, G. N.; Young, C. G. *J. Am. Chem. Soc.* **2000**, *122*, 2946−2947.
(11) Rappe, A. K.; Goddard, W. A., Jr. *J. Am. Chem. Soc.* **1982**, *104*, 3287−3294.
(12) Peitsch, M. A.; Hall, M. B. *Inorg. Chem.* **1996**, *35*, 1273−1278.
(13) Thomson, L. M.; Hall, M. B. *J. Am. Chem. Soc.* **2001**, *123*, 3995−4002.
(14) Izumi, Y.; Glaser, T.; Rose, K.; McMaster, J.; Basu, P.; Enemark, J. H.; Hedman, B.; Hodgson, K. O.; Solomon, E. I. *J. Am. Chem. Soc.* **1999**, *121*, 10035−10046.
(15) Frisch, M. J.; Trucks, G. W.; Schlegel, H. B.; Scuseria, G. E.; Robb, M. A.; Cheeseman, J. R.; Zakrzewski, V. G.; Montgomery, J. A., Jr.; Stratmann, R. E.; Burant, J. C.; Dapprich, S.; Millam, J. M.; Daniels, A. D.; Kudin, K. N.; Strain, M. C.; Farkas, O.; Tomasi, J.; Barone, V.; Cossi, M.; Cammi, R.; Mennucci, B.; Pomelli, C.; Adamo, C.; Clifford, S.; Ochterski, J.; Petersson, G. A.; Ayala, P. Y.; Cui, Q.; Morokuma, K.; Malick, D. K.; Rabuck, A. D.; Raghavachari, K.; Foresman, J. B.; Cioslowski, J.; Ortiz, J. V.; Stefanov, B. B.; Liu, G.; Liashenko, A.; Piskorz, P.; Komaromi, I.; Gomperts, R.; Martin, R. L.; Fox, D. J.; Keith, T.; Al-Laham, M. A.; Peng, C. Y.; Nanayakkara, A.; Gonzalez, C.; Challacombe, M.; Gill, P. M. W.; Johnson, B. G.; Chen, W.; Wong, M. W.; Andres, J. L.; Head-Gordon, M.; Replogle, E. S.; Pople, J. A. *Gaussian 98*, revisions A6 and A7; Gaussian, Inc.: Pittsburgh, PA, 1998
(16) The DFT calculations were performed using Gaussian 98[15] with the B3LYP hybrid functional. The 6-31G basis set was used for carbon and hydrogen, while the 6-31G** was used for oxygen and sulfur. The LANL2DZ basis set and the LANL2 pseudopotentials of Hay and Wadt[20] were used for Mo. An optimization was performed in C_1 symmetry, and a frequency calculation yielded no imaginary frequencies, confirming that a global minimum had been obtained.
(17) Garrett, R. M.; Johnson, J. L.; Graf, T. N.; Feigenbaum, A.; Rajagopalan, K. V. *Proc. Natl. Acad. Sci. U.S.A.* **1998**, *95*, 6394−6398.
(18) McNaughton, R. L.; Tipton, A. A.; Rubie, N. D.; Conry, R. R.; Kirk, M. L. *Inorg. Chem.* **2000**, *39*, 5697−5706.
(19) Lim, B. S.; Willer, M. W.; Miao, M.; Holm, R. H. *J. Am. Chem. Soc.* **2001**, *123*, 8343−8349.
(20) (a) Hay, P. J.; Wadt, W. R. *J. Chem. Phys.* **1985**, *82*, 270−283. (b) Wadt, W. R.; Hay, P. J. *J. Chem. Phys.* **1985**, *82*, 284−298.

JA017217T